Expanding Underground. Knowledge and Passion to Make a Positive Impact on the World – Anagnostou, Benardos & Marinos (Eds)

Investigation of microfine cement both rheological properties and permeation in soils

K. Boschi
DICA, Politecnico di Milano, Milan, Italy
DISAT, Bicocca University, Milan, Italy

R.P. Castellanza
DISAT, Bicocca University, Milan, Italy

C.G. di Prisco
DICA, Politecnico di Milano, Milan, Italy

D. Grassi
Master Builders Solutions, Treviso, Italy
DISAT, Bicocca University, Milan, Italy

ABSTRACT: Permeation grouting, i.e. injections at low pressure, of microfine cements is frequently adopted in tunnelling and underground structures to either increase the mechanical properties or reduce the hydraulic conductivity of soils. From an applicative point of view, the time dependent permeation process, crucial to assess the spatial contour of the final content of the injected microfine cement, is highly affected not only by operational parameters, geometry of injection sources and particulate phase nature of the grout under exam, but also by its time-dependent rheological properties. This latter aspect is not deeply investigated in literature, especially in the ranges of shear rates, times and water-cement ratios commonly adopted during permeation grouting treatments. To this aim, in this paper, a comprehensive investigation has been performed, combining laboratory experiments with theoretical approaches. The time-dependent rheological properties of microfine cements characterized by different water-cement ratios have been first quantified by means of rheometric tests and described with a Bingham's law. The microfine cement permeation in granular media has then been experimentally investigated and so the employment of a Darcy's law modified to incorporate the temporal evolution of Binghamian grout rheologies has been validated for microfine cement flows.

1 INTRODUCTION

Permeation grouting of microfine cements is a technique commonly employed in tunnelling and underground structures. It consists in injecting at controlled low-pressure values a fluid-like material which in turn permeates throughout the soil voids. After microfine cement curing, a treated soil with larger strength and stiffness and reduced hydraulic conductivity is obtained. More precisely, microfine cements are suspensions of particles in a fluid medium, analogous to ordinary portland cement. However, the mean particle size of microfine cements is about one order of magnitude smaller than that of ordinary portland cements (with grain sizes ranging from 63 to 0.1 μm), resulting in better flow properties and bleeding characteristics (De Paoli et al., 1992). When employed in permeation grouting applications, they are observed to flow sufficiently through soils with hydraulic conductivity (K) values higher than 10^{-5} m/s (Kirsch & Bell, 2012). Christodoulou

DOI: 10.1201/9781003348030-185

et al. (2009) performed laboratory 1D injection tests by employing microfine cements and then the grouted soil cylindrical specimens were subjected to undrained triaxial compression tests. The following observations were derived: (i) the increase in cement fineness improves the groutability of cement suspensions rendering them effective for grouting of medium to fine sands; (ii) a satisfactory reduction (3 to 5 orders of magnitude) in permeability of sands can be obtained by grouting with microfine cement suspensions and the permeability reduction increases with sand grain size; (iii) in terms of strength improvement, grouting with micro- or ultra-fine cements offers a significant advantage over the coarser cements with the same chemical composition.

However, an accurate prediction of the time dependent permeation process in soils is first crucial to assess the spatial contour of the final content of injected microfine cement and it is highly affected not only by operational parameters, geometry of injection sources (Boschi et al., 2022b) and particulate phase nature of the grout (Boschi et al., 2022a) under exam, but also by its time-dependent rheological properties. Especially this latter aspect is not deeply investigated in literature, considering the ranges of shear rates, times and water-cement ratios commonly adopted during permeation grouting treatments. Christodoulou et al. (2009) themselves were the ones who firstly observed that predictive tools of groutability employing "groutability ratios" between characteristic sizes of injected soil and grout, present in literature and often employed in practise, are too optimistic. Few years ago, Mozumder et al. (2018), by injecting microfine cement grouts in sand columns, observed that also the other approaches present in literature to evaluate microfine cement injectability in soils (Markou et al., 2015; Yoon & El Mohtar, 2013) do not consider the high influence played by the actual grout rheology, until now erroneously assumed as Newtonian and time-independent. More precisely, they developed artificial neural network (ANN) and support vector machine (SVM) based penetrability prediction models to identify the key variables in groutability predictions and to quantify their effects.

In this paper, with the ambition of more-deeply understanding the phenomena occurring during permeation grouting governed by complex chemo-mechanical couplings, a different approach has been followed. In Paragraph 2, the time-dependent rheological properties of commercial microfine cements characterized by different water-cement ratios have been first quantified by means of rheometric tests and described with the Bingham's rheology. Then, the employment of a Darcy's law modified to incorporate the temporal evolution of Binghamian rheologies (Boschi, 2022; Boschi et al., 2022c) has been proposed to simulate more accurately microfine cement flows in soils (Paragraph 3). In the same paragraph, referring to already-published numerical results based on a discrete element method (Boschi et al., 2020; 2022a), an indication in terms of maximum particulate phase characteristic size of the grout to be employed has been also provided. Moreover, a predictive tool for feasibility studies and design phases of permeation grouting treatments, already proposed by Boschi (2022) and Boschi et al. (2022c) for nanosilicate grouts and based on the modified Darcy's law, has been also recalled for MC grout injections. In Paragraph 4, the proposed approach has been validated against experimental 1D injection test results.

2 RHEOLOGY OF MICROFINE CEMENTS

To better characterise the rheological behaviour of microfine cement (MC) grouts, a commercially available MC (MasterRoc MP 650; MBS Italia, 2021) was employed in laboratory. Its characteristics, as supplied by the manufacturer, are: as for the particle size distribution (PSD), 30 μm diameter refers to 98% passing, 15 μm to 94%, 5 μm to 44%, 2 μm to 16% and blaine fineness BF = 625 m^2/kg. Ordinary tap water was mixed with this MC to prepare fresh MC grouts characterised by water-cement (w/c) ratios ranging between 0.8 and 1.2 (by weight of dry MC). A fixed superplasticizer (Glenium Sky 421) dosage of 1% by weight of dry MC was also added to enhance the flow properties, as commonly done in practical applications.

The temporal evolution of MC grout rheological properties, characterized by different w/c ratios, were quantified by means of rheometric tests. First of all, the fresh grouts were accurately prepared in laboratory by employing a high-speed mixer for a total mixing time of few minutes. More precisely, the chosen superplasticizer dosage was firstly mixed with water thoroughly. Then, the specified amount of dry MC was added in small increments with 70% of the

superplasticizer-mixed water, while agitating the suspension continuously. Then, after the addition of the remaining 30% superplasticizer-mixed water, the grout suspension attained the specified w/c ratio and was subjected to continuous agitation until the actual rheometric test started. To perform these tests, Thermo Scientific HAAKE Viscotester iQ rheometer was employed with a 4-blade vane and a grooved vessel (according to Shamu & Håkansson, 2019). A constant rotational velocity and so shear rate $\dot{\gamma}$, ranging between 10 and 120 s^{-1}, was imposed to the vane, whereas the torque moment was measured continuously with time as well as shear stress τ. System temperature T was kept constant and equal to 20°C. Stable and repeatable τ measures were so taken and presented hereafter.

Thanks to these results, the change of rheological properties of a MC grout with time during hydration (Rahman et al., 2015) is firstly discussed in Paragraph 2.1, in particular with reference to the grout with w/c = 0.8. Then, in Paragraph 2.2, the influence played by the w/c ratio in the temporal evolution of MC rheological properties is highlighted.

2.1 *Time-dependent constitutive relationship*

In Figure 1a, the temporal evolution of τ vs. $\dot{\gamma}$ curves for the tested w/c = 0.8 MC grout is reported (different symbols refer to different time instants, being 0 the time instant at which grout suspension attained the target w/c ratio at the end of the mixing phase). Looking at the time sequence for any tested $\dot{\gamma}$ value, a progressive increase in τ, due to the occurrence of chemical reactions within the material, is evident; the growth, being relatively smooth at the beginning, becomes more pronounced thereafter.

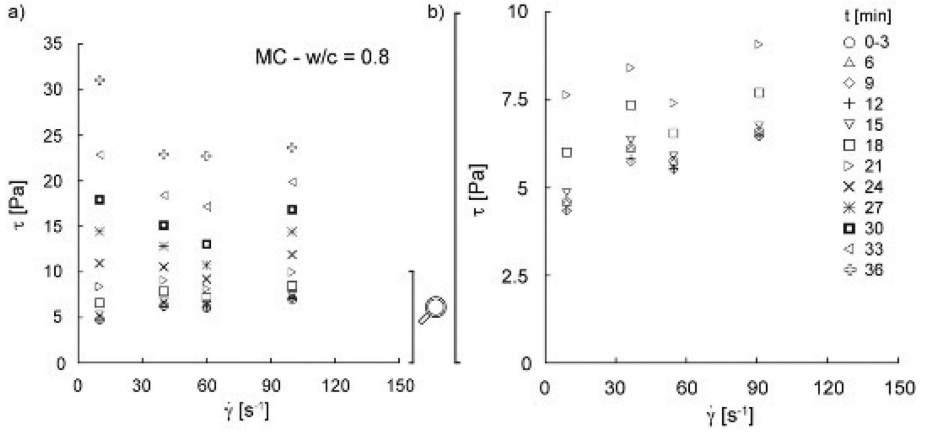

Figure 1. MC grout with w/c = 0.8: a) τ vs. $\dot{\gamma}$ curves derived from rheometric tests; b) magnification of a) for $t < t_{RFA}$.

While initially the τ vs. $\dot{\gamma}$ evolution for a fixed time instant can be interpreted as monotonic, after more or less 24 minutes, according to the research of Shamu & Håkansson (2019) focusing on the steady flows of cementitious suspensions, two different regions can be identified. An unstable region and a homogenous flow one are marked by an inflection point, defined at the minimum τ for a critical $\dot{\gamma}$. In the unstable flow region, below the critical $\dot{\gamma}$, the material within the rheometer is no longer uniformly sheared due to flow localisations, with coexisting sheared fluid material as well as un-sheared bands of material in a solid-like regime. A negatively sloped branch in the τ vs. $\dot{\gamma}$ is so observed below the critical $\dot{\gamma}$ and its slope increases with time, suggesting that some significant structural build-up occurs. In the homogenous flow region, above the critical $\dot{\gamma}$, the material inside the rheometer is uniformly sheared, without localisation, behaving as a fluid-like material. The time at which these two regions start coexisting is assumed to coincide with t_{RFA} after which the grout changes its consistency into a solid and permeation in soils is inhibited.

For the sake of clarity, in Figure 1b, a magnification of Figure 1a for $t < t_{RFA}$ is added. As was already observed by many authors for cementitious grouts in general (Håkansson et al., 1992;

Pantazopoulos et al., 2012; Markou et al., 2015), it is evident that, for a fixed time instant t, such that $0 < t < t_{RFA}$, the MC grout rheological behaviour can be described by a Bingham's rheology ($\tau = \tau_0 + \mu \cdot \dot{\gamma}$) with the coexistence of both viscosity μ and yield stress τ_0. Once the experimental data (Figure 1b) for each time instant are interpolated by means of the linear Binghamian relationship, curves $\tau_0(t)$ and $\mu(t)$ can be derived to describe the time dependency of the grout rheology (squares of Figures 2a and 2b, respectively). These trends detect that w/c = 0.8 MC grout behaves like a fluid with fixed both τ_0 and μ for times lower than $t^*_{w/c=0.8}$. Thereafter, solidification phase starts and yield stress prevails, by increasing rapidly. The initial viscosity of the fluid, one order of magnitude higher than the one of both water and nanosilica grouts (Boschi, 2022), instead, decreases rapidly (thixotropic behaviour), reaching a value close to 0 at $t = t_{RFA}$, when an unstable flow region starts coexisting with the stable one and playing a not-negligible role.

2.2 *Influence of water-cement ratio*

Additional w/c ratios, commonly employed in permeation grouting applications (1 and 1.2), were tested in addition to the w/c = 0.8 case previously examined. The time evolutions of both $\tau_0(t)$ and $\mu(t)$ for these two additional w/c ratios are compared always in Figure 2. It is evident that:

- from a qualitative point of view, the evolution with time of both τ_0 and μ are slightly dependent on w/c ratios: constants until a time t* and then t_0 rapidly increasing as well as μ rapidly decreasing until t_{RFA};
- higher the w/c ratio is, lower the initial value of τ_0 is;
- for w/c = 0.8, the initial value of μ is two times the ones referred to w/c ≥ 1, with these latter close to 10 mPa·s;
- t_{RFA} slightly depends on w/c ratio, being on the order of 20 min in all the examined cases.

Then, it can be concluded that, in permeation grouting applications, the choice of a higher w/c ratio associated with lower initial both τ_0 and μ values would be preferable during the injection phase itself. Being aware that lower w/c ratios are expected to be more effective from a mechanical viewpoint, the choice of a higher w/c ratio would be also economically convenient.

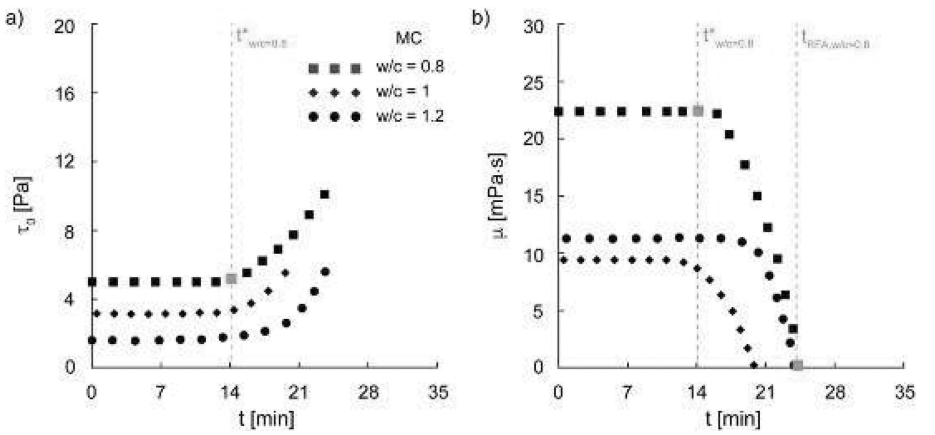

Figure 2. Functions a) $\tau_0(t)$ and b) $\mu(t)$ related to different microfine cement (MC) grouts at various w/c ratios.

3 MODELLING OF MICROFINE CEMENT FLOWS THROUGHOUT SOILS

To simulate flows of time-dependent Binghamian fluids throughout soils, Boschi (2022) and Boschi et al. (2022c) have recently presented a modified Darcy's law and validated it when dealing with nanosilica grouts. This is expressed as

$$v(t) = -K(t) \cdot \left\langle 1 - \frac{G(t)}{\gamma} \frac{1}{||i(t)||} \right\rangle \cdot i(t), \tag{1}$$

where the Macaulay brackets ⟨-⟩ evaluate to zero for negative arguments, returning the argument itself if positive; $v(t)$ is the grout seepage velocity, $K(t) = k \cdot \gamma/\mu(t)$ the hydraulic conductivity with k [m^2] the soil intrinsic permeability and γ the grout weight per unit volume, $i(t)$ the hydraulic gradient, $||i(t)||$ its modulus and $G(t)/\gamma$ the minimum hydraulic gradient for the flow to be triggered. This last term is strictly related to the Binghamian nature of the fluid under exam and directly depends on not only fluid τ_0(t) parameter but also characteristic dimension of the soil pore matrix. Indeed, $G(t)$ is expressed as

$$G(t) = \frac{16}{3} \cdot \frac{\tau_0(t)}{d}, \tag{2}$$

where d is identified by the authors as the mean pore throat diameter of the soil. Gueven et al. (2017) provided an accurate estimation of d value as a function of n and average particle size diameter D_{50} in the case of quite poorly-dispersed spherically-shaped granular media: $d = (0.1808\ n + 0.0069) \cdot D_{50}$. Alternatively, Kenney et al. (1985) estimated diameter d_p of the largest particles that can permeate throughout the porous matrix of a soil under exam, as a function of its coefficient of uniformity C_u and fine fraction dimensions D_5 and D_{15} (Figure 3). Being pore throats the narrowest void areas of the porous matrix coincident with pore restrictions, the d_p value is strictly related to the d one and Figure 3 can be employed to estimate the d value to be inserted into Equation 2.

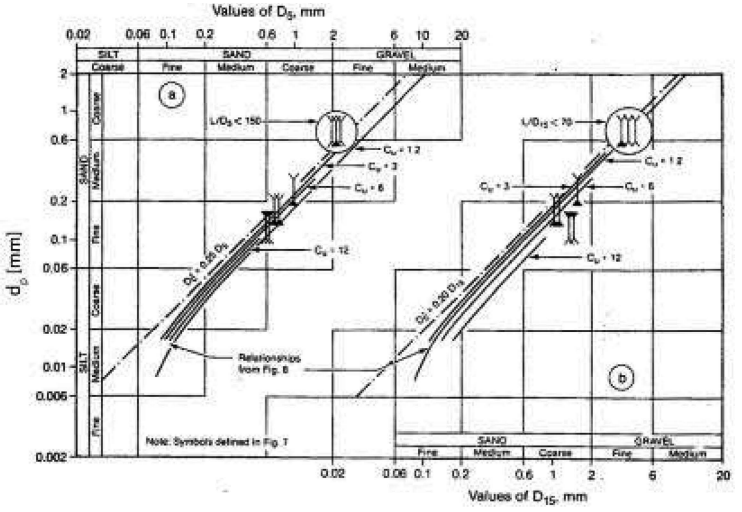

Figure 3. Diameter of the largest particle potentially transported throughout the soil matrix d_p as a function of soil fine fraction sizes (D_5 and D_{15}) and coefficient of uniformity Cu (modified figure from Kenney et al., 1985).

The proposed $v(t)$ vs. $i(t)$ relation is expected to correctly capture time-dependent Binghamian MC grout permeation throughout soils, as will be validated in Paragraph 4, but only when it is not affected by the particulate phase characteristic length itself. Indeed, the MC particulate phase could act as a barrier during MC grout advancement in soils when it is characterised by dimensions comparable or higher than soil void ones, until enhancing clogging of MC particles, resulting in permeation of grout fluid phase only, leaving behind the particulate one ("filter-cake" phenomena). However, these events want to be prevented in practical applications for not undermining the treatment effectiveness, so a sufficiently fine MC, with respect to the soil about to be treated,

has to be chosen during the design phase and then Equation (1) can be employed to predict MC grout advancement evolution.

Recently, thanks to numerical results based on a discrete element method, Boschi et al. (2020; 2022a) have concluded that, in order to prevent any unwanted MC grout advancement dependence upon particulate phase characteristic length, the particulate phase characteristic size cannot overcome more or less 1/2 d_p of the soil (Figure 3).

Boschi (2022) and Boschi et al. (2022c) have firstly employed this just-introduced modified Darcy's law to obtain closed-form solutions for permeation of time-dependent Binghamian grouts in soils starting from either spherical or cylindrical injection sources. They are based on the following main simplifying assumptions (Boschi et al., 2022b; 2022c): (i) constant soil porosity n and k both in space and with time, (ii) immiscibility of fluids (injected and interstitial ones), (iii) negligibility of gravity and capillarity effects, (iv) flow laminar regime, according to the so called sharp-front model and (v) head losses to be concentrated in the injected grout, being the injected fluid more viscous than the interstitial one. In the spherical case, constant flow rate to be imposed Q^*, radius attained by the injected fluid front r_g and applied injection pressure p_{inj} are observed to be related through the following system of equations:

$$\begin{cases} \langle p_{inj}(t) - G(t) \cdot (r_g(t) - r_0) \rangle - \frac{Q^* \mu(t)}{4\pi k} \cdot \left(\frac{1}{r_0} - \frac{1}{r_g(t)} \right) = 0 \\ r_g(t) - r_0 \cdot \sqrt[3]{1 + \frac{3Q^*}{4\pi n r_0^3} \cdot t} = 0, \end{cases} \tag{3}$$

where r_0 is the radius of the injection source. These equations may be applied to obtain the whole injection characteristic curves, i.e. the evolutions with time of p_{inj} and r_g, given an imposed flow rate, resulting in an useful predictive tool for feasibility studies and design phases of permeation grouting treatments (Boschi et al., 2022d).

4 VALIDATION OF MODIFIED DARCY'S LAW FOR MICROFINE CEMENT FLOWS

The MC grout front advancement in sand has then been experimentally investigated (Paragraph 4.1). Thanks to the comparison with the derived experimental 1D injection test results, the employment of the modified Darcy's law (Equation 1) and of the consequently proposed predictive tool have been validated when dealing with MC grouts.

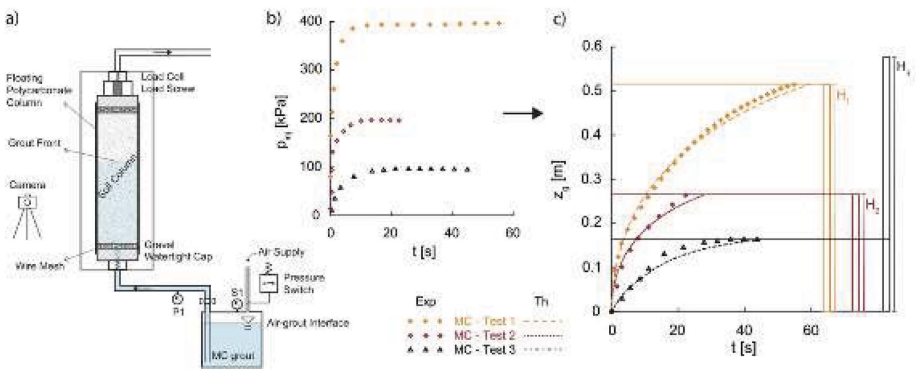

Figure 4. A) Experimental set-up for injection experiments; b) imposed p_{inj} evolutions with time t; c) MC grout front advancement z_g derived by means of camera acquisitions.

4.1 *Experimental tests and results*

To detect grout front advancements in soils with time, the apparatus for 1D injection tests, shown in Figure 4a and described in Boschi (2022) and Grassi (2022), was designed and hereinafter

employed. A series of dry Hostun sand specimens inserted into a floating polycarbonate column were initially subjected to a fixed confining pressure, through the load screw located at the top boundary. Then, they were injected from the bottom boundary by imposing a prescribed p_{inj} temporal evolution, monitored by means of a pressure transducer located at the bottom boundary. Grout front advancements z_g were detected with time by means of camera acquisitions. The experimental campaign was performed by changing $p_{inj}(t)$ and the height of the specimen of Hostun sand (D_{10} = 275 mm, D_{50} = 375 mm, n = 0.41, k = $5 \cdot 10^{-11}$ m^2), whereas the MC grout injected was unique (w/c = 1, γ = 15 kN/m^3, $\mu(t)$ and $\tau_0(t)$ reported in Figure 2) and p_c = 600 kPa (any change in p_c for sufficiently large values, not allowing the nullification of force chains, is expected not to affect the injection process since the tested sand is characterised by a C_u = 1.4).

The experimental results (symbols) reported in Figures 4c are so obtained by imposing the $p_{inj}(t)$ illustrated in Figure 4b to specimens of different heights (column height H_1 = 52 cm in Test 1, H_2 = 27 cm in Test 2 and H_3 = 56 cm in Test 3). In Figure 4c, on the right, the heights of each sand specimen are reported: as is evident, in case of Tests 1 and 2, the injection of the sand specimen is complete, since the grout front gets the top of the specimen. In case of Test 3, the front does not get the top, since the maximum p_{inj} imposed is not sufficient to allow any further front advancement. It is worth recalling that the material rheology is changing with time and the local gradient is progressively decreasing for increasing values of z_g. The authors, in order to be sure that such an arrest in the front advancement is not due to material curing, imposed a further increase in the p_{inj} and they observed (the corresponding data are here omitted for the sake of simplicity) a further increase in z_g.

4.2 *Numerical simulations*

First of all, it is worth noticing that, for the sand under exam and according to Figure 3, $d_p \sim$ 35 μm, whose value, compared with the MC grout PSD, guarantees these experimentally performed grout front advancements not to be affected by the MC particulate phase characteristic length. These MC grout injections in Hostun sand are so analytically reproduced by considering the same simplifying assumptions employed by Boschi et al. (2022c) to derive System of Equation 3, but referred, in this case, to a linear 1D seepage geometrical condition, and so by imposing:

$$n \cdot \frac{dz_g(t)}{dt} = \frac{k}{\mu(t)} \cdot \left\langle \frac{p_{inj}(t)}{z_g(t)} - \frac{16}{3} \cdot \frac{\tau_0(t)}{d} \right\rangle. \tag{4}$$

All the required input data values have been already provided (Paragraph 4.1, Figures 2 and 4b), except for d parameter, that is equal to 30.5 μm according to Gueven et al. (2017) relation (Paragraph 3). The analytically derived z_g temporal evolutions (lines) are compared with the

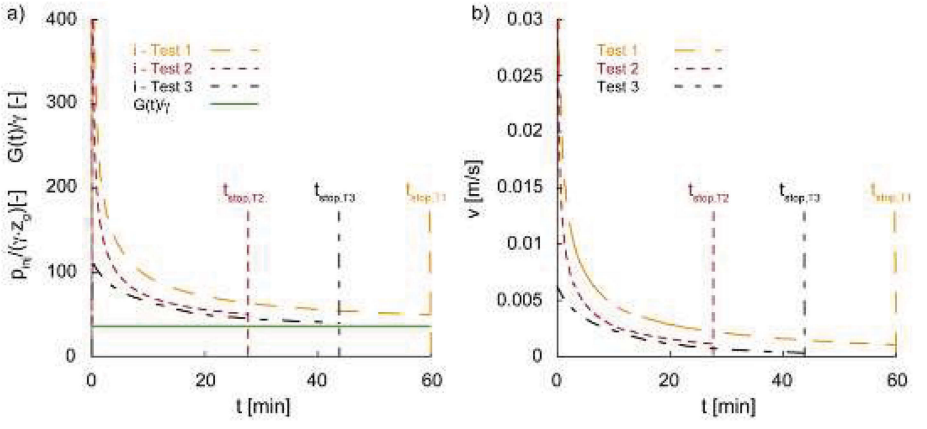

Figure 5. Numerical evolutions of a) hydraulic gradient $i = p_{inj}/(\gamma z_g)$, its triggering value $G(t)/\gamma$ and b) grout seepage velocity v referred to the three experimental tests simulated.

correspondent experimental data (symbols) in Figure 4c and the agreement is very satisfactory. In Figure 5, the analytically derived evolutions of both hydraulic gradients and grout seepage velocities are also reported. As is clear in Equation 4 and shown in Figure 5, the grout front stops in the middle of the column (Figures 4c and 5b; Test 3) only when the hydraulic gradient, that is $p_{inj}(t)/(z_g(t)\cdot\gamma)$ decreasing with time since $\dot{z}_g(t)>0$, almost equalizes $G(t)/\gamma$, which instead remains constant during the test time intervals ($0 < t < t_{stop}$; Figure 5a). It is worth mentioning that these results, for this p_{inj} investigated range, also common in practical applications, (i) have been verified by Boschi (2022) not to be significantly influenced by gravity effects and (ii) turn out to be highly affected not only by grout rheology but also by d parameter (Boschi, 2022). Finally, in the light of these observations, the authors suggest to suitably design permeation grouting treatments especially in terms of p_{inj} value to be imposed, e.g. employing System of Equation 3, in order to avoid any premature MC grout flow stoppage.

5 CONCLUSIONS

In this paper, key factors affecting permeation of microfine cement (MC) grouts in soils have been investigated. First of all, an accurate rheological characterization of MC grouts, commonly employed in permeation grouting treatments, has been provided. Then, the employment of a predictive tool for feasibility studies and design of permeation grouting treatments with MC grouts, based on the definition of a modified Darcy's law capable of taking into account the role played by the time-dependent Binghamian rheology, has been successfully validated. This has been possible thanks to experimental results, in terms of front advancement evolutions, of one-dimensional MC grout injection tests, performed into sand columns by imposing different values of injection pressures. This predictive tool allows to correctly reproduce the MC grout arrest due to (i) an imposed injection pressure too low with respect to the grout yield stress and the soil mean pore throat diameter and (ii) grout solidification process.

In this paper, the "filter-cake" phenomena were not taken into account since the MC grout was treated as a flowing continuum and its particulate nature was neglected. Nevertheless, the authors have recalled that the relation between maximum particulate phase characteristic size of the grout to be employed and fine fraction sizes of the soil to be treated has been already provided by them in a previous work, employing a discrete element method numerical code.

ACKNOWLEDGEMENTS

This research was funded by MBS Master Builders Solutions Italia S.p.A. within a research program aimed at both investigating and modelling the coupled hydro-mechanical processes governing grout injections.

REFERENCES

Boschi, K., di Prisco, C. G., & Ciantia, M. O. (2020). Micromechanical investigation of grouting in soils. International Journal of Solids and Structures, 187, 121–132.

Boschi, K. (2022). Permeation grouting in granular materials. From micro to macro, from experimental to numerical and viceversa. PhD Thesis. Politecnico di Milano. http://hdl.handle.net/10589/182992

Boschi, K., Ciantia, M. O., & Di Prisco, C. G. (2022a). Pressure grouting of microfine cements in soils: micromechanical processes. In 20th International Conference on Soil Mechanics and Geotechnical Engineering (pp. 621–626). Australian Geomechanics Society.

Boschi, K., Grassi, D., Castellanza, R., & di Prisco, C. (under review – 2022b) Permeation Grouting in Soils: Numerical Investigation and Modelling. Proceedings of the Institution of Civil Engineers – Ground Improvement.

Boschi, K., di Prisco, C., Grassi, D., Modoni, G. & Salvatore, E. (2022c). Permeation grouting con sospensioni di silice colloidale in terreni granulari. Incontro Annuale dei Ricercatori di Geotecnica IARG 2022. Volume ISBN 9788897517108.

Boschi, K., Arroyo, M., Burbano, D.A. & Spagnoli, G. (2022d). Permeation grouting of an upstream tailing dam: a feasibility study. Proceedings of Tailings & Mine Waste 2022 Conference.

Christodoulou, D. N., Droudakis, A. I., Pantazopoulos, I. A., Markou, I. N., & Atmatzidis, D. K. (2009). Groutability and effectiveness of microfine cement grouts. In Proceedings of the 17th International Conference on Soil Mechanics and Geotechnical Engineering (Volumes 1, 2, 3 and 4) (pp. 2232–2235). IOS Press.

De Paoli, B., Bosco, B., Granata, R., & Bruce, D. A. (1992). Fundamental observations on cement-based grouts (2): Microfine cements and the Cemill® process. In Grouting, Soil Improvement and Geosynthetics (pp. 486–499). ASCE.

Grassi, D. (2022). Tecnologie innovative per il consolidamento di substrati di fondazione e opere geotecniche. PhD Thesis. Bicocca University. https://boa.unimib.it/handle/10281/366246

Håkansson, U., Hässler, L., & Stille, H. (1992). Rheological properties of microfine cement grouts. Tunnelling and Underground Space Technology, 7(4),453–458.

Yoon, J., & El Mohtar, C. (2013). Groutability of granular soils using sodium pyrophosphate modified bentonite suspensions. Tunnelling and Underground Space Technology, 37, 135–145.

Kenney, T. C., Chahal, R., Chiu, E., Ofoegbu, G. I., Omange, G. N., & Ume, C. A. (1985). Controlling constriction sizes of granular filters. Canadian Geotechnical Journal, 22(1),32–43.

Kirsch, K., & Bell, A. (Eds.). (2012). Ground improvement. CRC Press.

Markou, I. N., Christodoulou, D. N., & Papadopoulos, B. K. (2015). Penetrability of microfine cement grouts: experimental investigation and fuzzy regression modeling. Canadian Geotechnical Journal, 52 (7),868–882.

MBS Italia. (2021). MasterRoc MP 650: Scheda Tecnica. https://www.master-builders-solutions.com/it-it/download-area?f=Brands$:#4d6173746572526f63&page=2

Mozumder, R. A., Laskar, A. I., & Hussain, M. (2018). Penetrability prediction of microfine cement grout in granular soil using Artificial Intelligence techniques. Tunnelling and Underground Space Technology, 72, 131–144.

Pantazopoulos, I. A., Markou, I. N., Christodoulou, D. N., Droudakis, A. I., Atmatzidis, D. K., Antiohos, S. K., & Chaniotakis, E. (2012). Development of microfine cement grouts by pulverizing ordinary cements. Cement and Concrete Composites, 34(5),593–603.

Rahman, M., Håkansson, U., & Wiklund, J. (2015). In-line rheological measurements of cement grouts: Effects of water/cement ratio and hydration. Tunnelling and Underground Space Technology, 45, 34–42.

Shamu, T. J., & Håkansson, U. (2019). Rheology of cement grouts: On the critical shear rate and no-slip regime in the Couette geometry. Cement and Concrete Research, 123, 105769.